Three dimensional cross-linked and flexible graphene composite paper with ultrafast electrothermal response at ultra-low voltage

Huicong Chang [a, *], Yi Jia [a], Lin Xiao [a], Honghui Chen [b], Kai Zhao [b], Yongsheng Chen [b], Yanfeng Ma [b, **]

[a] Qian Xuesen Laboratory of Space Technology, China Academy of Space Technology, Beijing, 100094, China
[b] State Key Laboratory and Institute of Elemento-Organic Chemistry, The Institute of Polymer Chemistry, College of Chemistry, Nankai University, Tianjin, 300071, China

ABSTRACT

Electro thermal papers have been widely applied in people's daily life. Compared to traditional metal alloy resistance heaters, three dimensional graphene/carbonized-PAN composite freestanding paper with lightweight, good flexibility and excellent electrothermal performance is presented. It retains intrinsic properties of graphene sheets in the bulk state, and exhibits fast electrothermal response under low operation voltage with robust mechanical property. The fastest specific heating rate could be up to $213\,°C\,s^{-1}\,V^{-1}$, and the highest T_s is $235\,°C$ at low driving voltage just of $1.75\,V$, which far surpasses those of previous carbon-based film heaters, commercial nichrome wire, and Kanthal wire. These outstanding properties together with the advantage of facile and large-scale fabrication, make the composite paper with great potential applications in flexible electronics.

© 2019 Elsevier Ltd. All rights reserved.

1. Introduction

Superior electrothermal heating elements own merits of high electrothermal conversion efficiency and fast electrothermal response and widely used in applications including vehicle window defrosters, outdoor display, household electric heater and other heating systems [1–3]. The traditional resistance heaters, such as Ni–Cr and Fe–Al alloys, are limited by their heavy weight, rigidity, intolerance to acids and bases and limited heating efficiency [4,5]. In general, ultrafast electrothermal response, low operation voltage, and good flexibility are the three key parameters to evaluate the efficiency of the electro-heating devices.

Graphene based materials, including 1D fiber and 2D film, are promising candidates for electrothermal heating elements due to its good electric and thermal properties [6–8]. Particularly, 2D films such as graphene based transparent films have been highly concerned as electrothermal heaters for vehicle window defrosters and heating retaining windows, due to their transparency and light weight [9–11]. However, such transparent electrothermal heaters usually need to attach to fragile substrate (glass or ITO) and could not form a large-scale film with uniform electrothermal properties. So it has highly limited their applications in many fields of large scale heating system and high power heating elements, such as home electric heating system, aircraft wing deicing system [5,12–14], which require a free-standing and lightweight macroscopic paper with fast thermal response and low operation voltage as possible.

Macroscopic graphene material maintained the 2D intrinsic properties of graphene sheets in the bulk state with high electrical and thermal properties is ideal electrothermal heaters. Moreover, low specific gravity, chemical resistance, large heating area and infrared radiation beneficial to human body are the unique advantages of the graphene electrothermal papers (GEPs). Various preparation methods have been developed to obtain GEPs such as chemical vapor deposition (CVD), vacuum filtration/thermal reduction, electrochemical exfoliation and ball-milling [15–18]. However, due to the defects of graphene sheets or/and the weak van der Waals interaction between graphene sheets after reduction process, these GEPs usually can't perform well both the electrothermal and the mechanical performance, with long response time up to stable-state temperature (beyond 10 s) and higher operation voltage (more than 10 V) [8,19–22]. Extensive efforts have been made to increase the interlayer interaction between graphene

---

* Corresponding author.
** Corresponding author.
 E-mail addresses: changhuicong@qxslab.cn (H. Chang), yanfengma@nankai.edu.cn (Y. Ma).

sheets via covalent crosslinking, hydrogen bonding, ionic bonding, and van der Waals attraction [23–28]. Generally, these external enhancers contain flexible polymer chains, metal ions binding, organic functional molecule and inorganic nano filler [29–33], which could remarkably improve the mechanical performance of the GPs, even give GPs some extra exciting performance. However, these external components would deteriorate the electrical property and the thermal stability of the GEPs. Thus, it's a great challenge to develop a macroscopic GEP, retaining intrinsic properties of graphene sheets in the bulk state, exhibiting fast electrothermal response under low operation voltage together with robust mechanical property.

2. Experimental

2.1. Preparation of three dimensional graphene (3DG)

The 3DG was prepared as following procedures. The starting material, graphene oxide (GO), was synthesized by the oxidation of natural graphite powder using a modified Hummers' method. 3DG was prepared following our previous procedures. The GO was dispersed in ethanol, and a low concentration GO solution (~0.5 mg mL^{-1}) was solvothermally treated in a Teflon-lined autoclave at 180 °C for 12 h. Then the as-prepared ethanol-filled intermediate product was carefully removed from the autoclave to have a slow and gradually solvent exchange with water. After the solvent exchange process was totally completed, the water-filled product was freeze-dried. Finally, the material was annealed at 400 °C for an hour in argon atmosphere to obtain the 3DG.

2.2. Preparation of 3DG/carbonized-PAN composite paper

For 50%PAN@3DG, first, 100 mg 3DG was dispersed in 50 mL DMF by stiring, then followed by adding 100 mg PAN dissolved in 10 mL DMF and the mixture solution was homogeneous through stiring. The mixture was concentrated by solvent evaporation at 70 °C, casted in teflon mold and then mechanical pressed at 270 MPa for 1 h to obtain the compact 3DG/PAN composite paper. The mechanical press was achieved in a stainless steel moulding, and then was pressed by a machine to achive certain pressure on the up and down surface of the mould. The mould effective size was 40 mm in diameter and 50 mm in height. The obtained paper was pre-oxidized under 20 MPa at 270 °C for 360 min in air and then carbonized under 20 MPa at 1000 °C and 1500 °C for 60 min in Ar atmosphere to obtain the final 3DG/carbonized-PAN composite paper. The press process at high temperature was obtained through two graphite cylindrical mold face to face at certain pressure and the pressure was kept by four graphite screw spike.

2.3. Characterization

The morphology of the 3D GPs was observed by scanning electron microcopy (Nova Nano SEM 230 operated at 5.0 kV). The X-ray photoelectron spectroscopy (XPS) analysis was obtained using PHI 5000 VersaProbe (ULVAC-PHI, Japan). Raman spectra were examined with a Renishaw InVia Raman spectrometer using laser excitation at 514.5 nm. Combustion elemental analysis (EA) was done at Vario Micro cube, (Elementar, Germany) for determination of the C, H and O content. The tension testing was carried out by single fiber tension machine with tension rate of 10 mm min-1 (LLY-06ED, Lai zhou electron instrument CO. LTD). The sample was cut into a strip of 20 × 3 mm^2 and the thickness of the samples were 30–60 μm. The electrical conductivity was measured by four-probe method using Keithley 2450. The electrothermal behavior of the 3D GPs was studied mainly on a rectangular sample

(5 × 20 mm^2) powered by a d. c. power supply (KA3005D/P), while the temperature of the sample was monitored using an infrared temperature detector (QC 300, Taicooen).

3. Result and discussion

Recently, we have developed a three dimensional crosslinked bulk graphene material (3DG) which possesses a homogeneous structure, with low density (near air) and close to 100% porosity, assembled by randomly oriented graphene sheets through covalent bonds [34–36]. We adopt a strategy of using this 3DG as precursor instead of traditional GO dispersion to prepare graphene paper, which, on one hand, would greatly avoid the long-time assembly layer by layer, more importantly, would increase the interaction between the graphene sheets by chemical bonding. The X-ray photoelectron spectroscopy (XPS) in Fig. S1 demonstrated the exsistence of C–O (~286.7 eV) and C=O (~288.6 eV) bonds. The peak at 1717 and 1190 cm^{-1} in the infrared spectrum (IR) in Fig. S2a are assigned to the stretching vibrations of C=O and C–O. The Scanning Electron Microscope (SEM) in Fig. S2b showed the crosslinking structure of 3DG. All these proved under the solvothermal synthesis conditions, reactions are expected among the OH, COOH and epoxy bond functional groups of adjacent graphene sheets to generate aromatic ether and ester bonds between the sheets. Furthermore, using polyacrylonitrile (PAN) derived structure (carbonized-PAN) as filler, as shown in Fig. 1a, an intercalated and compact 3DG/carbonized-PAN composite paper was obtained through mechanical press, peroxidation and carbonization. The sp^2 graphite domains from carbonized-PAN were filled in the voids of 3DG and provided transport paths for the electrons in basal plane of graphene. Meanwhile, they acted as structure enhancer to increase the interaction between the graphene sheets to improve the mechanical and electrical performance of the whole composite papers.

By varying the content of PAN occupying the voids of the 3DG, an optimal balance between compactness and electrons prior transfer channel would be achieved. The tension strength and electrical conductivity increased with the addition of PAN until 50%, as shown in Fig. S3. The optimized composite paper was 50% PAN@3DG-1500 with addition of 50 wt% PAN and carbonized at 1500 °C. It exhibited excellent electrical and mechanical performance (tension and bending performance). The optimized composite paper by carbonized-PAN filling improved the tension strength to 52 MPa, increasing 85% compared with the pure 3DG paper (Fig. 1b), and was ten times more than the commercial graphite paper (Fig. 1b). The specific electrical conductivity (κ/ρ, κ is the electrical conductivity (S m^{-1}) and ρ is density (g cm^{-3})) of optimized composite paper was 1×10^5 S m^{-1}, increasing 150% compared with the pure 3DG paper (Fig. S3b) and was same order magnitude with traditional Ni–Cr and Fe–Al alloys resistance heaters (~10^5 S m^{-1}). Further increasing the fraction of PAN beyond 50% led to encasing the 3DG skeleton in the carbonized-PAN graphite domains after high temperature annealing. On one hand, this resulted in the fracture point transferring from 3DG to graphite domain and weakened mechanical performance. On the other hand, the carbonized-PAN dominated in the composite film, resulting more grain boundaries between the graphene and smaller graphite domains of carbonized-PAN. Electrons would be hindered when transport between these domains, resulting lower electrical conductivity than the optimized composite paper. Compared with other graphene based papers in literatures [7,17,18,37,38] (Fig. 1c), the optimized composite paper furthest retained the intrinsic graphene properties, combining both the mechanical and electrical performance.

Graphene based materials are attractive for energy-efficient electro thermal heaters because of their low heat capacity,
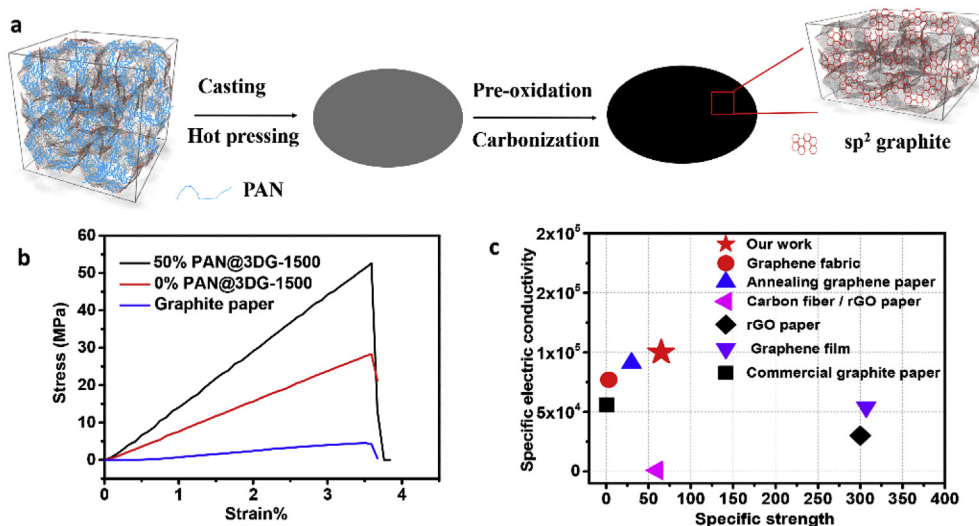
Fig. 1. (a) The schematic diagram of preparation process of the 3DG/carbonized-PAN composite paper. **(b)** Strain-stress curve of the optimized composite paper (50%PAN@3DG) and pure 3DG paper without PAN, both carbonized at 1500 °C and commercial graphite paper. **(c)** Comparison of the specific electrical conductivity and specific tension strength of the optimized composite paper with other graphene based papers in literature. Specific electrical conductivity is defined as κ/ρ, where κ is the electrical conductivity (S m^{-1}), ρ is density of the paper (g cm^{-3}). Specific tension strength is defined as σ/ρ, where σ is the tension strength (MPa). (A colour version of this figure can be viewed online.)

excellent joule heating performance. Advantage of above excellent electrical and mechanical performance of the optimized graphene composite paper made it promise as electro thermal heater. Both ends of the optimized graphene composite electrothermal paper (OGEP) were connected to a direct current power supply by copper foil. The temperature distribution of the paper under an electric field was monitored by a real time infrared thermal detector. As illustrated in Fig. S4, when the electric field was carried out, both the heating and cooling process accomplished within 1 s until the corresponding saturated temperature (T_s) was reached. This fast thermal response owed to the low thermal capacity of the OGEP compared to other materials. The T_s of the OGEP were 65, 97, 125

and 196 °C at input voltage of 0.88, 1.13, 1.30 and 1.61 V, respectively (Fig. 2a). Moreover, both the T_s and heating rate linearly rise with input voltage (Fig. 2b). Considering the higher T_s in literatures was obtained at higher voltage, the specific heating rate (heating rate/ voltage) was defined for fair comparison. Compared with rGO film and CNT film in literatures [7—9,20,39], even commercial heating element and carbon fiber paper, the OGEP showed fastest specific heating rate and higher T_s, as shown in Fig. 2c. The fastest specific heating rate could be up to 213 °C s^{-1} V^{-1}, and the highest T_s was 235 °C at low driving voltage just of 1.75 V, which far surpasses those of previous carbon-based film heaters, commercial nichrome wire, and Kanthal wire.
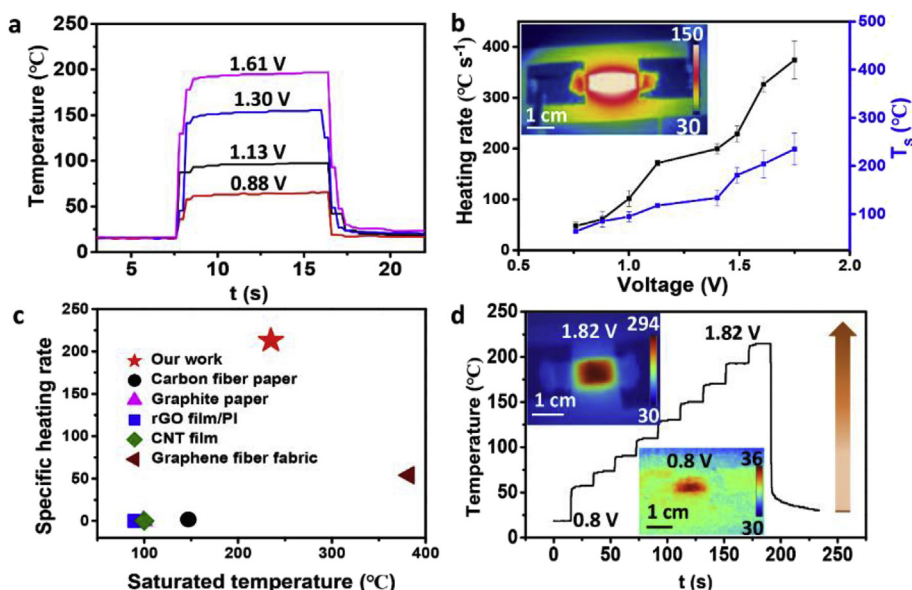

Fig. 2. (a) Temperature profiles of the optimized composite paper at different applied voltage. **(b)** Heating up rate and the corresponding saturated temperature as a function of the input voltage for the optimized composite paper. Insert is its infrared image at the input voltage of 1.4 V. **(c)** Comparison of the specific heating rate and saturated temperature of the optimized composite paper with other carbon based materials in literatures. Specific heating rate is defined as heating rate divided by applied voltage **(d)** Temperature profiles of the optimized composite paper under stepwise voltage from 0.8 V to 1.82 V. Insert are the infrared images at the input voltage of 0.8 and 1.82 V. All the scale bar above were 1 cm. (A colour version of this figure can be viewed online.)

When applied a voltage on the paper, the temperature was uniformly distributed at the whole paper (insert of Fig. 2b), indicating the structure integrity and homogeneity of the OGEP. Furthermore, the OGEP showed fast responsibility and without hysteresis when worked in periodic or stepwise process. As illustrated in Fig. 2d, with stepwise voltage from 0.80 to 1.82 V applied to the paper, the temperature rise up accompanied with the increasing input voltage and the temperature distribution was uniform (insert of Fig. 2d). This indicated the structure integrity and easy to operation of the OGEP. The surface temperature distribution was measured and recorded with infrared camera.

It was the first reported carbon based material to have such fast specific heating rate at lower driving voltage. Such outstanding electro thermal performance ascribed to the unique microstructure of the 3DG filled by the carbonized PAN with low thermal capacity [40]and excellent electrical and thermal properties. When a fixed voltage was applied on the OGEP, the electrons would transport between the domains of the paper at the external electric field. This lead to interaction between electrons and lattice at numerous grain boundaries and finally the electric-thermal energy exchange. In such pure resistance circuit, Ohm's law ($U = IR$) and Joule's law ($Q = I^2 Rt$)) were applicative. Theoretically, assuming the electrical energy has been completely converted to thermal energy, the conversion could be described by Joule's law $P = U^2/R$ (where P is the input electric power, U is the input voltage and R is the resistance of the sample). At a constant DC voltage, a smaller R means more electric energy converted to thermal energy, which was in accordance with the excellent electric conductivity of the OGEP. The density of the OGEP is less than 1.0 g cm^{-1} (Fig. S5), much lower than commercial graphite paper (~1.8 g cm^{-1}) and traditional rGO paper obtained by filtration or exfoliation method (1.5—2.5 g cm^{-1}). According to the relationship of thermal energy and temperature, $dQ = cmdT$, where dQ is the thermal energy change, dT is the temperature change, c, m are the thermal capacity and mass of the sample, respectively, the OGEP had low thermal capacity and much lower density, so much higher T_s and faster response could be obtained at constant voltage circuit (Fig. S6).

The microstructure of the OGEPs was investigated by scanning electron microscope (SEM). The section morphology of the pure 3DG-1500, 50%PAN@3DG-1500 papers and pure PAN-1500 fragments (Fig. 3a—c) showed that the composite papers densified with larger PAN content. The pure 3DG-1500 paper remained the original 3D crosslinked structure and retained parts of the voids (Fig. 3a), and the pure PAN-1500 displayed smooth and homogeneous morphology but can't form an integrated paper due to the high inner stress during carbonization process (Fig. 3c). While the 50%PAN@3DG-1500 presented compact structure with the carbonized-PAN domains almost entirely filling the voids and interlocking the graphene sheets (as marked by red dash line in Fig. 3b). And finally it formed an integrated composite paper as shown in insert of Fig. 3b. The carbonized PAN (graphite domains) filling the voids of the 3DG afforded extra electron transport channels and strengthen the interaction of graphene sheets.

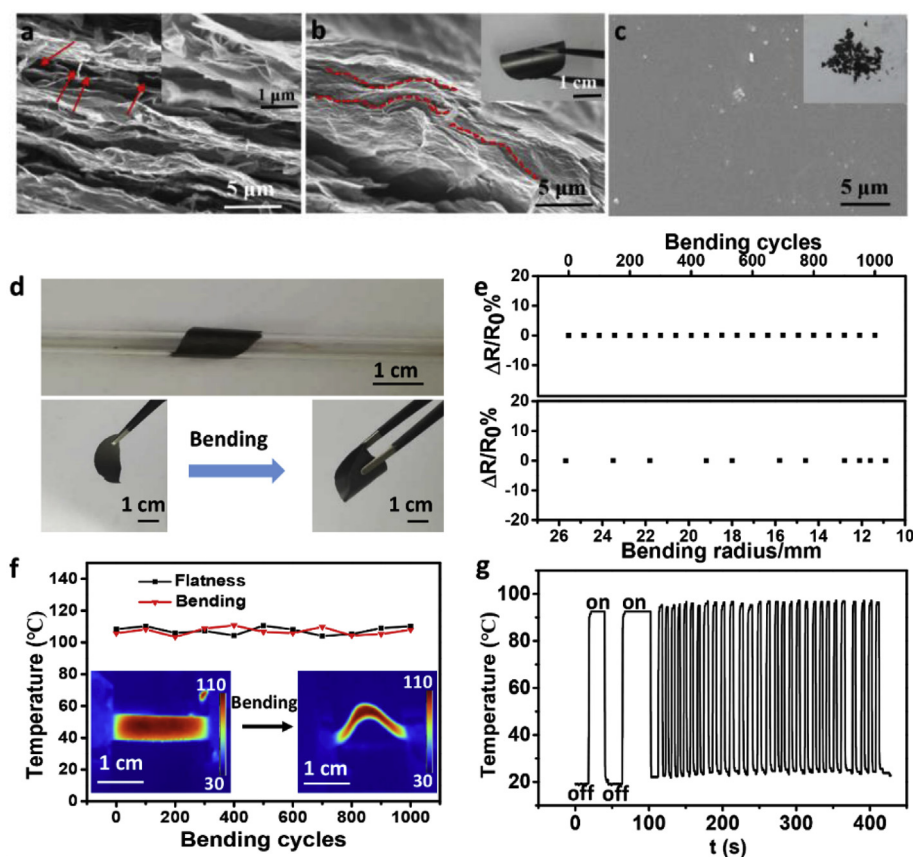Furthermore, high carbonization temperature made effective

Fig. 3. (a) The cross-section SEM of pure 3DG paper carbonized at 1500 °C. Insert is the high magnification with the 3D crosslinked structure. The cross-section SEM of **(b)** the optimized composite paper with 50% PAN content and **(c)** 100% PAN fragments. The scale bar above is 5 μm. Inserts are the photographs of the macro papers respectively. **(d)** Photographs of different bending state of the optimized composite paper. **(e)** Electrical-resistance variation of the optimized composite paper at bending radius up to 10 mm and under cyclic bending for 1000 times. **(f)** The temperature evolution of the optimized composite paper under 1000 bending cycles at voltage of 1.0 V. Insert are the infrared images of the paper in a bending cycle. **(g)** The cyclic stability of the optimized composite paper during 500 cycles between on and off at driving voltage of 1.0 V. All the scale bar above were 1 cm. (A colour version of this figure can be viewed online.)
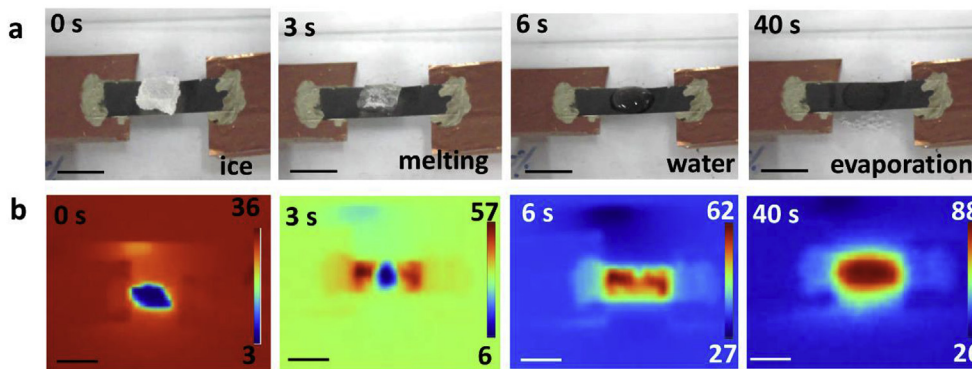
Fig. 4. (a) Photographs of the ultrafast deicing process. The ice (~7 × 4 × 4 mm^3, 30 mg) was absolutely melted in 6 s and further evaporated in 40 s. **(b)** The corresponding infrared images of the deicing process in panel (a). All the scale bar above were 1 cm. (A colour version of this figure can be viewed online.)

restoration of the conjugated structure of the graphene and graphite domains to improve its electrical performance. X-ray photoelectron spectroscopy (XPS) and elemental analysis (EA) showed the N atoms almost removed (Fig. S7) and carbon content sharply increased with the temperature increasing from 1000 °C to 1500 °C (Table S1). Furthermore, the increase of sp^2 crystalline domain size (L_a, in-plane size and L_c, out-plane size) also demonstrated the restoration of the sp^2 structure with the increasing temperature (Figs. S8 and S9, Tables S2 and S3). And the graphite domains possible grow along the edge defect of graphene sheets to improve the mechanical performance (Figs. S10 and S11). Thus, the specific electrical conductivity of the composite paper was in the same order of magnitude with traditional metal alloys for electro-thermal heaters.

Based on above structure analysis, the combination of 3DG and PAN could make up their respective shortcomings. On one hand, the voids of 3DG would provide adequate space to disperse the inner stress of the graphite domains from carbonized-PAN. On the other hand, the graphite domains would intercalate the graphene sheets to be favorable for electrical and mechanical properties. Fig. 3d show the excellent bending performance of OGEP. We investigated its bending behavior by monitoring the variation of electrical resistance. The resistance didn't change dramatically with the variation of bending radius (Fig. 3e), suggesting a good tolerance on bending deformation. After 1000 bending-releasing cycles for a radius of 18 mm, the resistance kept stable without obviously variation (Fig. 3e). Such excellent bending performance was also shown in electrothermal conversion process. As shown in Fig. 3f, no obvious temperature change was observed after 1000 bending cycles (curve radius of 18 mm). The temperature distribution of the flatness and bending papers was uniform from infrared images of insert of Fig. 3f, demonstrating the mechanical thermal stability of the OGEP. Moreover, the paper exhibited fast response between on and off at driving voltage of 1.0 V. The T_s kept steady even after 400 cycles (Fig. 3g). Such mechanical, specially bending stability under heating process was due to the 3D crosslinked micro structure of the 3DG/carbonized-PAN composite paper. Also, the excellent electrothermal performance under bending proved its wide application under harsh environment.

Moreover, the OGEP exhibited an outstanding dehumidification and deicing ability. As shown in Fig. 4, a piece of ice (~7 × 4 × 4 mm^3, 30 mg) is entirely melted rapidly within 6 s at 1.0 V on a rectangular paper (20 × 5 × 0.035 mm^3). And within 40 s, the melted water completely evaporated. From the infrared images of the paper under deicing process, the temperature of the paper gradually was uniform with the ice melting and the water evaporation. The rapid response for deicing and the weather resistance of

the carbon made the composite paper a promising candidate in the large-area and quick heating field.

4. Conclusion

In conclusion, using 3DG and carbonized-PAN as skeleton and filler respectively, we have developed a novel composite graphene paper, which exhibited outstanding specific electrical conductivity up to 1×10^5 S m^{-1}. Furthermore, the composite paper demonstrated excellent electro-thermal properties with the fastest specific heating up rate per voltage of 213 °C s^{-1} V^{-1} and the T_s of 235 °C at low driving voltage just of 1.75 V, obviously better than commercial metal alloys, carbon fiber paper and graphite paper. Such excellent performance was attributed to its hierarchical structure with the graphite domains fully intercalating the voids of 3DG, serving as the bridge of graphene sheets to increase the transmission paths for the electrons. We believe the composite graphene paper have provided new thinking for the large-area and quick heating field.

Appendix A. Supplementary data

Supplementary data to this article can be found online at https://doi.org/10.1016/j.carbon.2019.08.008.

References

[1] T.J. Kang, T. Kim, S.M. Seo, Y.J. Park, H.K. Yong, Thickness-dependent thermal resistance of a transparent glass heater with a single-walled carbon nanotube coating, Carbon 49 (4) (2011) 1087—1093.

[2] R. Wang, Z. Xu, J. Zhuang, Z. Liu, L. Peng, Z. Li, et al., Highly stretchable graphene fibers with ultrafast electrothermal response for low-voltage wearable heaters, Adv. Electron. Mater. 3 (2) (2017).

[3] A.R. Griffin, A. Vijayakumar, R.H. Chen, K.B. Sundaram, L.C. Chow, Development of a transparent heater to measure surface temperature fluctuations under spray cooling conditions, J. Heat Transf. 130 (11) (2008) 1617—1620.

[4] M.K. Sinha, S.K. Mukherjee, B. Pathak, R.K. Paul, P.K. Barhai, Effect of deposition process parameters on resistivity of metal and alloy films deposited using anodic vacuum arc technique, Thin Solid Films 515 (4) (2006) 1753—1757.

[5] Z.P. Wu, J.N. Wang, Preparation of large-area double-walled carbon nanotube films and application as film heater, Phys. E Low-dimens. Syst. Nanostruct. 42 (1) (2010) 77—81.

[6] P.-C. Hsu, X. Liu, C. Liu, X. Xie, H.R. Lee, A.J. Welch, et al., Personal thermal management by metallic nanowire-coated textile, Nano Lett. 15 (1) (2015)

365—371.

[7] Z. Li, Z. Xu, Y.J. Liu, R. Wang, C. Gao, Multifunctional non-woven fabrics of interfused graphene fibres, Nat. Commun. 7 (2016) 11.

[8] D. Janas, K.K. Koziol, Rapid electrothermal response of high-temperature carbon nanotube film heaters, Carbon 59 (2013) 457—463.

[9] D. Sui, Y. Huang, L. Huang, J. Liang, Y. Ma, Y. Chen, Flexible and transparent electrothermal film heaters based on graphene materials, Small 7 (22) (2011) 3186—3192.

[10] Y.H. Yoon, J.W. Song, D. Kim, J. Kim, J.K. Park, S.K. Oh, et al., Transparent film heater using single-walled carbon nanotubes, Adv. Mater. 19 (23) (2007) 4284—4287.

[11] J. Yan, Y.G. Jeong, Highly elastic and transparent multiwalled carbon nanotube/polydimethylsiloxane bilayer films as electric heating materials, Mater. Des. 86 (2015) 72—79.

[12] J. Kang, H. Kim, K.S. Kim, S.-K. Lee, S. Bae, J.-H. Ahn, et al., High-performance graphene-based transparent flexible heaters, Nano Lett. 11 (12) (2011) 5154—5158.

[13] C. Li, Y.T. Xu, B. Zhao, L. Jiang, S.G. Chen, J.B. Xu, et al., Flexible graphene electrothermal films made from electrochemically exfoliated graphite, J. Mater. Sci. 51 (2) (2016) 1043—1051.

[14] J. Luo, H.F. Lu, Q.C. Zhang, Y.G. Yao, M.H. Chen, Q.W. Li, Flexible carbon nanotube/polyurethane electrothermal films, Carbon 110 (2016) 343—349.

[15] S. Pei, J. Zhao, J. Du, W. Ren, H.M. Cheng, Direct reduction of graphene oxide films into highly conductive and flexible graphene films by hydrohalic acids, Carbon 48 (15) (2010) 4466—4474.

[16] G. Xin, H. Sun, T. Hu, H.R. Fard, X. Sun, N. Koratkar, et al., Large-area free-standing graphene paper for superior thermal management, Adv. Mater. 26 (26) (2014) 4521—4526.

[17] H. Chen, M.B. Müller, K.J. Gilmore, G.G. Wallace, D. Li, Mechanically strong, electrically conductive, and biocompatible graphene paper, Adv. Mater. 20 (18) (2010) 3557—3561.

[18] Q.Q. Kong, Z. Liu, J.G. Gao, C.M. Chen, Q. Zhang, G. Zhou, et al., Hierarchical graphene—carbon fiber composite paper as a flexible lateral heat spreader, Adv. Funct. Mater. 24 (27) (2014) 4222—4228.

[19] R. Wang, Z. Xu, J. Zhuang, Z. Liu, L. Peng, Z. Li, et al., Highly stretchable graphene fibers with ultrafast electrothermal response for low-voltage wearable heaters, Adv. Electron. Mater. 3 (2) (2017).

[20] H. Im, E.Y. Jang, A. Choi, W.J. Kim, T.J. Kang, Y.W. Park, et al., Enhancement of heating performance of carbon nanotube sheet with granular metal, ACS Appl. Mater. Interfaces 4 (5) (2012) 2338—2342.

[21] F.X. Wang, K. Zhang, W.Y. Liang, Z.Q. Wang, B. Yang, Experimental and analytical studies on the flexible, low-voltage electrothermal film based on the multi-walled carbon nanotube/polymer nanocomposite, Nanotechnology 30 (6) (2019) 11.

[22] H. Huang, P. He, T. Huang, S. Hu, T. Xu, H. Gu, et al., An electrochemical strategy for flexible and highly conductive carbon films: the role of 3-dimensional graphene/graphite aggregates, ACS Appl. Mater. Interfaces 11 (1) (2019) 1239—1246.

[23] Q. Cheng, L. Jiang, Z. Tang, Bioinspired layered materials with superior mechanical performance, Accounts Chem. Res. 47 (4) (2014) 1256.

[24] A. Z, C. OC, P. KW, B. LC, N. ST, Bio-inspired borate cross-linking in ultra-stiff graphene oxide thin films, Adv. Mater. 23 (33) (2011) 3842—3846.

[25] W. Cui, M. Li, J. Liu, B. Wang, C. Zhang, L. Jiang, et al., A strong integrated strength and toughness artificial nacre based on dopamine cross-linked graphene oxide, ACS Nano 8 (9) (2014) 9511—9517.

[26] S. Eigler, M. Enzelberger-Heim, S. Grimm, P. Hofmann, W. Kroener, A. Geworski, et al., Wet chemical synthesis of graphene, Adv. Mater. 25 (26) (2013) 3583—3587.

[27] M.W. Tian, Y.N. Hao, L.J. Qu, S.F. Zhu, X.S. Zhang, S.J. Chen, Enhanced electrothermal efficiency of flexible graphene fabric Joule heaters with the aid of graphene oxide, Mater. Lett. 234 (2019) 101—104.

[28] X.J. Su, H.Q. Li, X.J. Lai, Z.P. Yang, Z.H. Chen, W.J. Wu, et al., Vacuum-assisted layer-by-layer superhydrophobic carbon nanotube films with electrothermal and photothermal effects for deicing and controllable manipulation, J. Mater. Chem. 6 (35) (2018) 11.

[29] K. Shahzadi, X. Zhang, I. Mohsin, X. Ge, Y. Jiang, H. Peng, et al., Reduced graphene oxide/alumina, a good accelerant for cellulose-based artificial nacre with excellent mechanical, barrier and conductive properties, ACS Nano 11 (6) (2017) 5717—5725.

[30] O.K. Park, C.S. Tiwary, Y. Yang, S. Bhowmick, S. Vinod, Q.B. Zhang, et al., Magnetic field controlled graphene oxide-based origami with enhanced surface area and mechanical properties, Nanoscale 9 (21) (2017) 6991—6997.

[31] X.J. Wu, Y. Wang, P. Yang, The field emission properties from the pristine/B-doped graphene-C-70 composite, Phys. Lett. A 381 (24) (2017) 2004—2009.

[32] D.M. Hu, W.B. Gong, J.T. Di, D. Li, R. Li, W.B. Lu, et al., Strong graphene-interlayered carbon nanotube films with high thermal conductivity, Carbon 118 (2017) 659—665.

[33] H.L. Li, S.C. Dai, J. Miao, X. Wu, N. Chandrasekharan, H.X. Qiu, et al., Enhanced thermal conductivity of graphene/polyimide hybrid film via a novel "molecular welding" strategy, Carbon 126 (2018) 319—327.

[34] Y. Wu, N. Yi, L. Huang, T. Zhang, S. Fang, H. Chang, et al., Three-dimensionally bonded spongy graphene material with super compressive elasticity and near-zero Poisson's ratio, Nat. Commun. 6 (2015) 6141.

[35] H. Chang, J. Qin, P. Xiao, Y. Yang, T. Zhang, Y. Ma, et al., Highly reversible and recyclable absorption under both hydrophobic and hydrophilic conditions using a reduced bulk graphene oxide material, Adv. Mater. 28 (18) (2016) 3504—3509.

[36] T. Zhang, H. Chang, Y. Wu, P. Xiao, N. Yi, Y. Lu, et al., Macroscopic and direct light propulsion of bulk graphene material, Nat. Photonics 9 (7) (2015).

[37] M. Zhang, Y. Wang, L. Huang, Z. Xu, C. Li, G. Shi, Multifunctional pristine chemically modified graphene films as strong as stainless steel, Adv. Mater. 27 (42) (2016) 6708—6713.

[38] Xin, H.T. Guoqing, F.R. Fard, Koratkar, et al., Large-area free standing graphene paper for superior thermal management, Adv. Mater. 26 (2014) 4521—4526.

[39] T.W. Lee, Y.G. Jeong, Regenerated cellulose/multiwalled carbon nanotube composite films with efficient electric heating performance, Carbohydr. Polym. 133 (2015) 456—463.

[40] J.H. Lehman, K.E. Hurst, A.M. Radojevic, A.C. Dillon, R.M. Osgood, Multiwall carbon nanotube absorber on a thin-film lithium niobate pyroelectric detector, Opt. Lett. 32 (7) (2007) 772—774.